A localization and updating strategy of large finite element models in structural dynamics

Cédric Pozzolini, Fabrice Buffe, Michel Salaün

A LOCALIZATION AND UPDATING STRATEGY OF LARGE FINITE ELEMENT MODELS IN STRUCTURAL DYNAMICS

C. POZZOLINI*, F. BUFFE*, M. SALAUN †

Keywords

Model updating, Error localization, Visibility, Constitutive Relation Error.

Abstract

The purpose of this paper is to evaluate the application of the error of constitutive law method to the updating of large FE models of space structures using FRF experimental results. First, we briefly recall the theoretical basis of this method in modal and frequency approaches. Then, the notion of visibility is introduced to improve the modelling of localization error and the quality of modal updating, for low frequencies. Finally we propose a global strategy and discuss the results we obtained on satellite JASON2.

1 Introduction

During the launch of a satellite, the level of excitation is very high. However, the security margins must be reduced in order to remain competitive. So CNES is concerned with the problem of Finite Element Model (FEM) updating in lower frequency to ensure that numerical simulations are predictive enough to maintain a high reliability of spacecraft structures. This problem has been a subject of intense research over the past twenty years, but the introduced methods are still hard to apply on industrial structures. Usually, the validation of a numerical dynamical model is performed by comparing numerical eigendata or Frequency Response Functions (FRF) with natural data measured from sine-sweep base excitation vibration tests. In FEM analysis, it is usual to make simplifying assumptions, in the modelling of joints for example, or to neglect some phenomena, such as contact between structures. Therefore, the purpose of modal updating is to modify parameters (such as mass, stiffness and damping of sub-structures or connections between components) in the numerical model in order to obtain better agreement between numerical and experimental data. To select erroneous parameters, a localization criterion is applied. It should be noted that the conditioning of the updating inverse problem is deteriorated when the number of erroneous parameters is too large or when the number of sensors is not large enough. That's why a sensitivity Monte Carlo analysis is used to remove non-significant parameters. Finally, the udapting process is assumed to be correct when the Modal Assurance Criterion (MAC) is accurate enough.

*Centre National d'Etudes Spatiales, 18 Avenue Edouard Belin, 31401 Toulouse, FRANCE. e-mail: cedric.pozzolini@cnes.fr, fabrice.buffe@cnes.fr

†Université de Toulouse, ISAE, 10 Avenue Edouard Belin, 31055 Toulouse, FRANCE. e-mail: michel.salaun@isae.fr

The modelling of error localization uses the existing error of constitutive law. In particular, the applicability of such a method to large industrial test cases such as JASON2 is adressed. In order to improve the quality of modal updating of the low frequency behaviour, a comparison between FRF and modal approaches of the error of constitutive law is made. Error location is extensively studied in the case of the dynamical behaviour of a clamped structure, with realistic limitations in order to find a better linear equivalent model. Design variables are typically thickness of panels and section or number of beams. Particular attention is paid to automatic selection of relevant parameters during updating in order to keep the sensitivity matrix well-conditioned and to obtain an accurate solution for parameters fitting.

2 Basics on error of constitutive law methods

The classical problem of linear elastodynamics to modelize a structure, which occupies a domain Ω of $\mathbb{R}^3$, is to find a displacement field u kinematically admissible (K.A.) and a stress $\boldsymbol{\sigma}$ such as

$$\forall v \text{ K.A. }, \int_\Omega f v d\Omega = \int_\Omega tr\Big(\boldsymbol{\sigma}(u)\boldsymbol{\varepsilon}(v)\Big)d\Omega - \int_\Omega \rho \frac{\partial^2 u}{\partial t^2} v d\Omega,$$

where ρ is the mass density and $\varepsilon(.)$ stands for the linearized strain tensor. The material constitutive law is $\boldsymbol{\sigma}(u) = \boldsymbol{H}\boldsymbol{\varepsilon}(u)$. In sine-sweep base forced vibration, boundary conditions are given, on a part Γ of $\partial\Omega$, by

$$\frac{\partial u}{\partial t}(.,t) = 0 \qquad u(.,t) = -\frac{a}{\omega^2}\sin(\omega t)$$

The associated discrete problem reads

$$[\mathbf{K}]u + i\omega[\mathbf{D}]u - \omega^2[\mathbf{M}]u = F \qquad (1)$$

where $[\mathbf{K}]$, $[\mathbf{D}]$ and $[\mathbf{M}]$ are respectively the stiffness, damping and mass matrices. For spacecraft structures, the damping is considered as small enough to use the so-called Basile hypothesis : $[\mathbf{D}] = \alpha[\mathbf{K}] + \beta[\mathbf{M}]$. Then, all these matrices depend on geometric and mechanical parameters (sections, thicknesses, Young modulus, Poisson ratio and density).

The Constitutive Relation Error (CRE) was initially proposed by Ladavèze *et al* in the early 1980's as an error estimator for FEM [3]. An extended version was described by Chouaki *et al* [1] in order to update mass, stiffness, and damping properties using the FRF data. In [**?**] is introduced a distance between two admissible displacement fields u and v in order to compare two different dynamical models of Ω. This distance in material constitutive law reads

$$d(u,v)^2 = \int_\Omega tr\Big(CL(u,v)\boldsymbol{H}^{-1}CL(u,v)\Big)d\Omega$$

where $CL(u,v) = \boldsymbol{\sigma}(u) - \boldsymbol{H}\boldsymbol{\varepsilon}(v)$.

In the industrial framework, we have a discrete numerical model of the structure and the measured data are a set of eigenmodes $\{\underline{\omega}_k^2 \ , \ \underline{u}_k\}_k$ or a set of displacement fields $\{\underline{u}_\omega\}_{\omega\in[\omega_{min},\omega_{max}]}$. Let us remark that these eigenvectors or displacement fields are only given at a few nodes of the mesh, more precisely where the sensors are located. So, the first step of the updating is to "expand" the measures to the full set of mesh nodes. In the case of an eigenmode $\{\underline{\omega}_k^2 \ , \ \underline{u}_k\}$ this expansion, say u_k , is the displacement field, denoted below by u, which minimizes the following function over the admissible displacements set

$$\begin{aligned} J_k(u,v,w) &= \tfrac{\gamma}{2}(u-v)^t[\mathbf{K}](u-v) \\ &+ \tfrac{1-\gamma}{2}(u-w)^t\underline{\omega}_k^2[\mathbf{M}](u-w) \\ &+ (\boldsymbol{\pi}u - \underline{u}_k)^t[\mathbf{K}]_{\boldsymbol{\pi}}(\boldsymbol{\pi}u - \underline{u}_k) \end{aligned}$$

$$\text{under the constraint } [\mathbf{K}]v = \underline{\omega}_k^2[\mathbf{M}]w. \qquad (2)$$

In this equation, $\boldsymbol{\pi}u$ denotes the restriction of u to the measured DOFs (sensors), while $[\mathbf{K}]_{\boldsymbol{\pi}}$ is the corresponding restriction of the rigidity matrix. Moreover, γ is a scalar parameter which value is generally taken as 0.5.

Remark 2.1. Let ϕ_k be the k^{th}-numerical mode: $[\mathbf{K}]\phi_k = \omega_k^2[\mathbf{M}]\phi_k$. Clearly, if $\underline{\omega}_k = \omega_k$ and $\underline{u}_k = \phi_k$, then $J_k(\phi_k,\phi_k,\phi_k) = 0$ and $u_k = \phi_k$, associated with $v_k = w_k = \phi_k$, is solution of the previous minimization problem.

For FRF data with damping, the expension of $\underline{u}_\omega$ is obtained by minimizing

$$\begin{aligned} J_\omega(u,v,w) &= \tfrac{\gamma}{2}(u-v)^t\big[[\mathbf{K}]+T\omega^2[\mathbf{D}]\big](u-v) \\ &+ \tfrac{1-\gamma}{2}(u-w)^t\omega^2[\mathbf{M}](u-w) \\ &+ (\boldsymbol{\pi}u-\underline{u}_\omega)^t[\mathbf{G}]_{\boldsymbol{\pi}}(\boldsymbol{\pi}u-\underline{u}_\omega) \end{aligned}$$

$$\text{such that } [\mathbf{K}]v+i\omega[\mathbf{D}]v-\omega^2[\mathbf{M}]w=F \tag{3}$$

where

$$[\mathbf{G}]_{\boldsymbol{\pi}}=\frac{\gamma}{2}[[\mathbf{K}]_{\boldsymbol{\pi}}+T\omega^2[\mathbf{D}]_{\boldsymbol{\pi}}]+\frac{1-\gamma}{2}\omega^2[\mathbf{M}]_{\boldsymbol{\pi}}\ ,$$

scalar T being a characteristic time, taken as the time length of measures for example.

Then, the updating problem belongs to the large class of inverse problems. To solve it, we assume that modelization errors are located where error of constitutive law is the highest. That's why an iterative algorithm is used, for which each iteration needs two steps: error location and correction. For this, we use a local indicator on each sub-structure of Ω, say Ω_i , which reads

$$\xi_i^2=\frac{1}{m}\sum_{k\le m}\Big[\sum_{el_i\in\Omega_i}\xi^2_{\underline{\lambda}_k,el_i}\Big]\quad ,$$

in which el_i stands for the finite elements belonging to Ω_i , the elementary terms being

$$\begin{aligned} \xi^2_{\underline{\lambda}_k,el_i} &= \tfrac{\gamma}{2}(u_k-v_k)^t[\mathbf{K}]^{el_i}(u_k-v_k) \\ &+ \tfrac{1-\gamma}{2}\underline{\omega}_k^2(u_k-w_k)^t[\mathbf{M}]^{el_i}(u_k-w_k) \end{aligned}$$

ξ_i can be normalized by the total energy on Ω, the local energy or the volume of Ω_i . A drawback of total energy normalization is that sub-structures with relatively small modeling errors but containing a large part of total structural energy may be associated with an indicator ξ_i much greater than a really erroneous sub-structure. For example, it can be the case when the number of sensors is relatively small. Then, the residual energy is spread over the structure and correctly modeled sub-structures with high energy may still be localized as erroneous.

The parameter correction process is typically performed by solving the non-linear optimization problem around (u_k,v_k,w_k) solutions of (2)

$$\begin{aligned} &\min_{p\in\mathcal{P}_j}\textstyle\sum_k \frac{\gamma}{2}(u_k-v_k)^t[\mathbf{K}](p)(u_k-v_k) \\ &+\tfrac{1-\gamma}{2}(u_k-w_k)^t\underline{\omega}_k^2[\mathbf{M}](p)(u_k-w_k) \\ &+(\boldsymbol{\pi}u_k-\underline{u}_k)^t[\mathbf{K}]_{\boldsymbol{\pi}}(p)(\boldsymbol{\pi}u_k-\underline{u}_k) \end{aligned} \tag{4}$$

where the sum is taken on all eigenmodes. p is a vector of active parameters, belonging to the set $\mathcal{P}_j$ defined at the j^{th} localization step. In a same way, for (u,v,w) solutions of (3), the minimization problem reads

$$\begin{aligned} &\min_{p\in\mathcal{P}_j}\textstyle\sum_{\underline{\omega}_k}\frac{1-\gamma}{2}(u-w)^t\underline{\omega}_k^2[\mathbf{M}](p)(u-w) \\ &+\tfrac{\gamma}{2}(u-v)^t\big[[\mathbf{K}](p)+T\underline{\omega}_k^2[\mathbf{D}](p)\big](u-v) \\ &+(\boldsymbol{\pi}u-\underline{u}_\omega)^t[\mathbf{G}]_{\boldsymbol{\pi}}(p)(\boldsymbol{\pi}u-\underline{u}_\omega) \end{aligned} \tag{5}$$

the sum being taken over the set of frequencies $\underline{\omega}_k$ which are identified with FRF in $[\omega_{min},\omega_{max}]$. It is important to note that the extended CRE formulation does not require a *a priori* pairing between analytical and experimental eigemodes. It is worth noticing that this last method has been tested only for small academic problems and not for industrial structures, such as JASON2.

3 Sub-structure visibility

This section deals with a generalization of visibility notion, introduced in [4]. Let us just remark that this quantity was introduced in the static case whereas we develop it for dynamics. For a given FEM, let n be the number of DOFs of the mesh, n_i the number of DOFs of sub-structure i, n_c the number of measured DOFs and n_{ss} the number of sub-structures. Then we introduce space $\mathcal{F}^i$, containing load vectors applied to DOFs of sub-structure i: more precisely, $\mathcal{F}^i$ is a n_i-dimensional subspace of $\mathbb{R}^n$, spanned by "unit vector fields" which values are 1 for one DOF of sub-structure i and 0 for all the others. Similarly, we define space $\mathcal{F}^c$, associated with loads applied to the measured DOFs: here again, $\mathcal{F}^c$ is spanned by "unit vectors" which values are 1 for one measured DOF and 0 for all the others. So it is clearly n_c-dimensional. Now, let us introduce space $\mathcal{U}^i$ of displacements due to any loading on i^{th}-sub-structure. Therefore, $\mathcal{U}^i$ is the image of $\mathcal{F}^i$ by $[\mathbf{K}]^{-1}$.

Our goal is to measure the sensors capability to localize defaults in material constitutive law on any sub-structure. In this respect, we introduce space $\mathcal{U}^{ck}$ such that

$$[\mathbf{Z}]_k(\mathcal{U}^{ck}) \;=\; \mathcal{F}^c \;\subset\; \mathbb{R}^n \quad ,$$

with $[\mathbf{Z}]_k \;:=\; [\mathbf{K}] - \omega_k^2[\mathbf{M}]$. So $\mathcal{U}^{ck}$ can be seen as set of displacement fields for which sensors are excited, in the case of the k^{th}-eigenmode. A measure of the visibility of sub-structure i for mode k is linked with the capability of space $\mathcal{U}^i$ to be properly represented by space $\mathcal{U}^{ck}$. For practical reasons, we denote by $[\mathbf{U}^{ck}]$ a matrix which columns are vectors of $\mathbb{R}^n$ generating a basis of space $\mathcal{U}^{ck}$: so $[\mathbf{U}^{ck}]$ is a rectangular matrix. Similarly, $[\mathbf{F}^c]$ is matrix of the unit vectors in each measured DOF (sensor). By definition of $\mathcal{U}^{ck}$, we have: $[\mathbf{Z}]_k[\mathbf{U}^{ck}] \;=\; [\mathbf{F}^c]$. Let us recall that matrix $[\mathbf{Z}]_k$ is singular. So column q of $[\mathbf{U}^{ck}]$, say $[\mathbf{U}^{ck}]_q$, is such that $[\mathbf{Z}]_k[\mathbf{U}^{ck}]_q \;=\; [\mathbf{F}^c]_p$ (p^{th}-column of $[\mathbf{F}^c]$). It is obtained through the classical formula

$$[\hat{\mathbf{U}^{ck}}]_q \;:=\; \sum_{j\neq k} \frac{\phi_j^\top\, [\mathbf{F}^c]_p}{\omega_j^2 - \omega_k^2}\, \phi_j \quad ,$$

which gives $[\mathbf{U}^{ck}]_q$ up to an element of the kernel of $[\mathbf{Z}]_k$, which is removed by

$$[\mathbf{U}^{ck}]_q \;:=\; [\hat{\mathbf{U}^{ck}}]_q \;-\; \left(\phi_k^\top\; [\mathbf{M}]\; [\hat{\mathbf{U}^{ck}}]_q\right) \phi_k \quad .$$

Then we set

Definition 3.1. The maximal dynamic visibility $\mathsf{V}^{\mathsf{ik}}{}_{\max}$ associated to i^{th}-sub-structure and k^{th}-mode is given by the ratio of energy induced by a perturbation on sensors DOFs of the i^{th}-sub-structure, by the total residual energy

$$\mathsf{V}^{\mathsf{ik}}{}_{\max} \;=\; \max_{x\in\mathbb{R}^n-\{0\}} \frac{x^\top[\mathbf{A}]x}{x^\top[\mathbf{B}]x} \quad ,$$

with $[\mathbf{A}] \;=\; ([\mathbf{U}^{ck}])^\top[\mathbf{K}]_i[\mathbf{U}^{ck}]$ and $[\mathbf{B}] \;=\; ([\mathbf{U}^{ck}])^\top[\mathbf{K}][\mathbf{U}^{ck}]$.

Let us remark that the size of matrix $[\mathbf{A}][\mathbf{B}]^{-1}$ is the number of sensors, then can be quickly computed. The visibility value belongs to the interval $[0, 1]$ and depends on sensors locations and on mode energy. A value of $\mathsf{V}^{\mathsf{ik}}{}_{\max}$ close to 0 ensure that a erroneous parameter is undetectable in the i^{th}-sub-structure, and can be neglected in the location error process. Conversely, $\mathsf{V}^{\mathsf{ik}}{}_{\max}$ close to 1 indicates that this sub-structure contributes significantly to the location process, for the error of constitutive law. Naturally, defining a frontier between "visible" and "unvisible" sub-structures is still an open problem, as it will appear in the following examples.

Remark 3.2. As in general matrix $[\mathbf{A}][\mathbf{B}]^{-1}$ is singular, the so-called minimal dynamic visibility $\mathsf{V}^{\mathsf{ik}}{}_{\min} := \min_x \frac{x^\top[\mathbf{A}]x}{x^\top[\mathbf{B}]x} = 0$, which explains this quantity is *a priori* useless.

4 Modal Updating of JASON2

To illustrate our strategy of localization/correction, we take the example of large FEM of JASON2 (weight 525 kg and 3 meters high), made of plate and shell elements assembled by beam elements, with a total of 50392 nodes and 302352 DOFs, see Fig. 1.

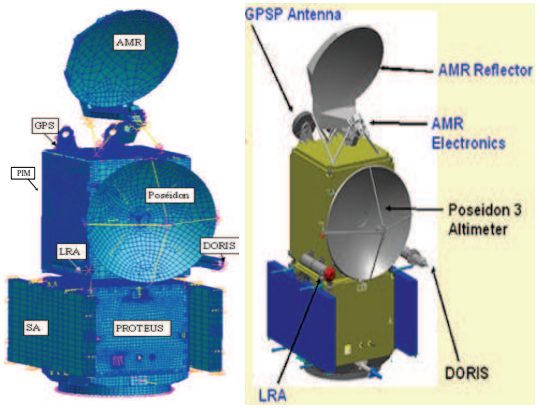

Fig.1 FEM JASON2

The modal and FRF CRE methods are implemented in AESOP software [2], which is developed by the LMARC Besançon. But very few numerical expenriences have been tested on the FRF CRE method. AESOP use SQP algorithm of Matlab to solve (4) or (5) , and the NASTRAN DEMAP.

EXP.		NUM. Initial			
Mode	Freq	Mode	Freq	Error	MAC
1	25.11	1	23.77	-5.35	86.8
2	26.48	2	24.91	-5.93	80.2
3	56.20	?5	54.51		~ 30
4	59.35	6	55.66	-6.21	82.8
5	61.28	7	57.08	-6.86	85.2
6	63.69	10	59.09	-7.22	95.9
7	64.43	16	69.49	7.85	77.0

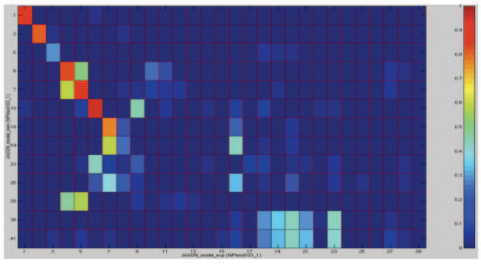

Fig.2 Initial MAC : Vertically (resp. horizontally) analytical (resp. experimental) modes are presented.

MAC coeff. $= \frac{(\boldsymbol{\pi}(\phi_i).\underline{u}_k)^2}{\|\boldsymbol{\pi}(\phi_i)\|\|\underline{u}_k\|}$

The vibration tests have been performed by ALCATEL in low frequency and around 87 modes were measured from 5Hz to 150Hz. In collaboration with the CNES, a new "multi-dofs" RTMVI (Real Time Modal Vibration Identification) method have been recently developed by TOPMODAL (Toulouse - France) in the software PRIMODAL [5]. Thanks to this method 29 experimental modes have been indentified, and the MAC have been calculated (Fig. 2).

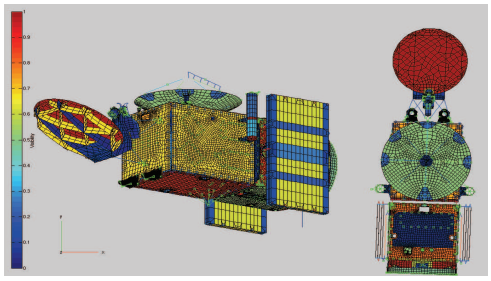

Fig.3 Static Visibility on 164 DOFs

We only select in the sum of formula (4) a set of modes with significant modal effective mass. We choose parameter associated to a good visibility zone of the model, to be sure that the sensors permit to see its erroneous. For the mode 1, the first step localization indicate the Pshell 151000 (in NASTRAN Model) lateral panel of PIM cube. But the updating investigation with thickness parameter fails in spite of a 0.64 static visibility. Ploting the error location by elements permits the identification of the most affected CQUAD elements. We noted the modeling error zones are very small and close to the interfaces of all lateral panels of PIM cube. The highest error, and visibility beams localized are properties Pbar 20000 and 18000, corresponding to the links the PROTEUS platform to PIM cube. By a Monte Carlo analysis we tested the sensitivity of area moment of inertia and the section of these beams. We note that mode 1 grows asymptocally as the inertia of the Pbar 20000. Finally an increase nearly ten time the area moment of inertia, three time the section of the Pbar 20000, and 1.8 time the section Pbar 18000, minimizes (4), and improves the correlation for the two firsts paired modes (see Fig. 6 and Fig. 7). The complex geometry of these elements confirmes your choice (see Fig. 4).

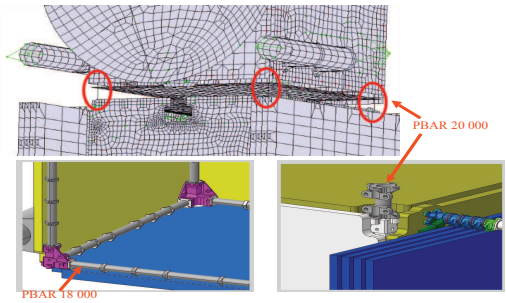

Fig.4 The complex geometry of pbar 20000 and 18000

Updating 1				Updating 2			
Mode	Freq	Error	MAC	Mode	Freq	Error	MAC
1	24.88	-0.91	86.3	1	25.1	0.01	86.4
2	26.48	-1.36	79.4	2	26.12	-0.5	79.6
5?	54.63		~ 30	5?	54.77		~ 30
6	56.07	-5.53	88.8	6	56.41	-5.41	88.1
8?	57.50		~ 70	8?	57.73		~ 65
9	59.14	-7.10	95.9	9	59.19	-7.07	95.6
16	69.51	7.88	77.3	16	69.51	7.89	77.2

Fig.5 JASON2 Updating Results

The second step's localization shows that the error is concentrated around the AMR

antenna (see Fig. 3). For the modes 2 to 7 the pbar 3050075 linking the AMR antenna to PIM are indicate, nevertheless they have low static visibility (0.2). Indeed the tickness updating of these beams do not improve the frequencies. To correct the the third mode (global vertical torsion) and the fourteenth mode (X-pumping) we take the thickness of Pshell 3050015 (AMR wire stretcher), it has the highest influence on the CRE, and 0.67 static visibility. A Monte Carlo run shows that the decrease of the thickness minimizes the CRE. We obtained a very good adjustment for the two firsts (Fig. 5) modes changing the Pshell 3050015 thickness from $0.001016m$ to $0.0008m$. However, one's again the error is localized in a small zone around local stiffeners as we can see on Fig.6.

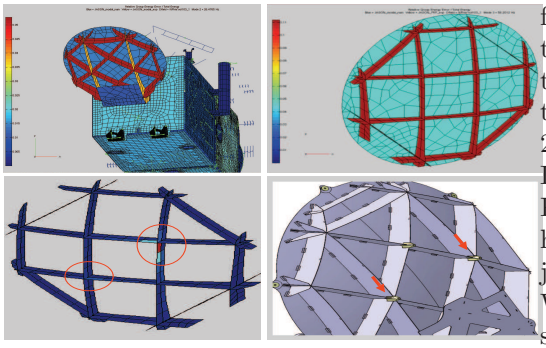

Fig.6 Localization : pshell 3050015 stiffener on AMR

We performed the same updating parameters with CRE FRF method. By comparing the FRF before and after adjustment parameters, we cleary see the improvement around the firts modes of the distance with the experimental function.

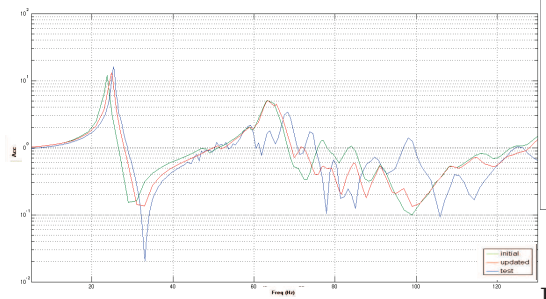

Fig. 7 JASON2 FRF comparison

Example 4.1. The model updating is usually limited to a correction of modal data, by changing the most sensitive parameters. We illustrate on the following example the difficulty to select a good parameter on the large FEM of JASON2, and We simulate an experimental model with 175 DOFs (sensors). There is no explicit relation between the extended CRE and the output errors that can be evaluated directly on the basis of the paired analytical and experimental eigensolutions. We modify the thikness of Pshell 12000, Pshell 151000 and section of Pbar 20000. Therefore we compare the intial and modified models, using the location process. In order to valid the extended CRE updating process on JASON2, we have tried various strategies to solve the (4) problem. On Fig. 8, Pshell 12000 and 151000 have good static visibility (0.99, both), but only 0.32 for Pbar 20000. In a first time, we have tried to find directly (without sensitivity analysis) the minimum of (4) with the three parameters of pshell 12000, Pshell 151000, and Pbar 20000 : the SQP algorithm did not converge. In a second time, we chosen to update only Pshell 12000 and Pshell 151000. After 27'34 hours running, we only optained a good adjustment for the Pshell 151000 parameter. We applied a Monte Carlo Latin Hypercube sensitivity analysis to the Pshell 12000 parameter. After 22'24 hours, the third updating corrected the three parameters, see Fig. 9.

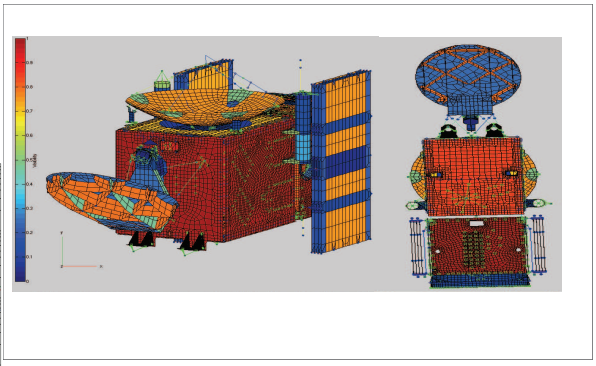

Fig.8 Static Visibility on 175 DOFs

Remark 4.2. The error estimator $J_k(u, v, w)$ defined in (2) grows when the term $(\boldsymbol{\pi} u - \underline{u}_k)^t [\mathbf{K}]_{\boldsymbol{\pi}} (\boldsymbol{\pi} u - \underline{u}_k)$ increases.

But there exists situation where $J_k(u, v, w)$ decreases and distance between ϕ_k and $\underline{u}_k$ grows. To illustrate this phenomenon, we consider the numerical updating problem defined in Example 4.1. However if we choose the thikness of the pshell 13000 to perform the updating, the design objective function (4) decreases while the error between the eigendata increases !

5 Conclusion

The CRE method is costly in large F.E. model to adjust parameters. The localization-correction cycle have to be repeated until no further improment is possible, but we do not know the global minimum of (4). Visibility function permits to select zone with significant error energy. How to use the visibility dynamic function to estimate the quality of the updating ? How the scalar factors in (4) influence the localization of dominantly erroneous subdomains ? There is not explicit relation between the extended CRE and the eigendata, however the location and number of sensors can damage the condition number of the (4) minimizing problem. We are now working on this line.

Data			Updating 2	Updating 3	
Property	Ini. Val.	Modif. Val.	Result 2	Monte Carlo Val.	Result 3
Pshell 12000	0.0012	0.004	0.00061	0.0009	0.00121
Pshell 151000	0.0012	0.003	0.00117	blocked	0.000119
Pshell 20000	0.0001849	0.0004	blocked	blocked	0.00028
CEE Ini. Cost : 0.38			CEE Cost 2 : 0.12	CEE Cost 3 : from 0.05 to 0.005	

Fig. 9 Numerical updating test on JASON2 with 175 DOFs.

References

[1] A. Chouaki, P. Ladevèze, L. Proslier, *Updating structural dynamic models with emphasis on the damping properties*, AIAA J., 36 (6), pp. 1094-1099, 1998.

[2] Cogan S., *AESOP. Analytical-Experimental Structural Optimization Platform* Version 5.0 User Guide

[3] Ladevèze P., Leguillon D., *Error estimate procedure in the finite element method and application*, SIAM J. Numer. Anal., 20 (3), pp. 485-509, 1983.

[4] S. Michot, *Contribution à la validation de modèles en dynamique des structures.* PhD Thesis, Université de Franche-Comté (spécialité sciences pour l'ingénieur), 2003.

[5] Roy N., *PRIMODAL An Innovative Software tool for Structural Dynamics in Industry* User's Manual Version 1.7